Alkanethiolate-Protected Copper Nanoparticles: Spectroscopy, Electrochemistry, and Solid-State Morphological Evolution †

ARTICLE *in* THE JOURNAL OF PHYSICAL CHEMISTRY B · SEPTEMBER 2001

Impact Factor: 3.3 · DOI: 10.1021/jp011280n

2 AUTHORS, INCLUDING:

Shaowei Chen
University of California, Santa Cruz
218 PUBLICATIONS **7,632** CITATIONS

SEE PROFILE

Alkanethiolate-Protected Copper Nanoparticles: Spectroscopy, Electrochemistry, and Solid-State Morphological Evolution†

Shaowei Chen* and Jennifer M. Sommers

Department of Chemistry, Southern Illinois University, Carbondale, Illinois 62901-4409

Received: April 6, 2001; In Final Form: June 27, 2001

Copper nanoparticles protected by alkanethiolate monolayers were prepared in a one-phase system using superhydride as the reducing reagent. The as-produced nanoparticles were typically found within the size range of 1−2 nm in diameter and of spherical shape. UV−vis and FTIR spectroscopies were carried out to investigate the particle optoelectronic properties and the molecular conformations of the protecting monolayers. Electrochemistry was used to study their quantized charging properties in solutions where the nanoparticle molecular capacitance was evaluated. When the particles were subject to mild-temperature thermal annealing in solid state, large (>10 nm) nanocrystals emerged with well-define facets and distinct surface morphologies. While the majority of the nanocrystals were spherical, other crystal shapes such as hexagons, pentagons, diamonds, triangles, and even rods were very visible. Discussion of the molecular mechanism for the shape evolution is presented.

Introduction

Nanometer-sized particles have been attracting extensive research interest, mainly due to the quantum effect by which the material properties are tunable by the particle size as well as the surface morphology.[1] Whereas it is most common to find nanoparticle molecules of spherical shapes, controlled synthesis of nanoparticles of other distinct surface morphologies can be accomplished by exploiting some unique organic/inorganic templates, where the resulting particles are embedded in the supporting matrixes. For instance, El-Sayed et al.[2] reported the synthesis of nanosized platinum particles capped by a polymer material, where tetrahedral, cubic, icosahedral, and cuboctahedral shapes were observed. Nonspherical palladium nanocrystals were generated in a surfactant/polymer gel[3] as well as in a tetra-*n*-octylammonium carboxylate supporting medium.[4] Using reverse micelles as microreactors and protecting shells, Pileni et al.[5] reported the synthesis of copper nanoparticles of varied shapes, whereas in dendrimer nanoreactors, typically only spherical copper nanoparticles were found.[6] More recently, Alivisatos et al. reported the synthesis of spherical and rod-shaped cobalt particles using a wet-chemistry approach at elevated temperatures.[7] Also, electrolytic techniques have been utilized to synthesize a variety of transition-metal colloids (e.g., gold, silver, palladium, nickel, and copper) of decahedral or icosahedral shapes by controlling the electrode potentials.[8] On the other hand, rod-shaped nanoparticles have been synthesized using electrolysis[9] as well as electrodeposition[10] techniques with surfactant or nanoporous membrane supports. More interestingly, Wang and co-workers recently demonstrated that nanosized belts of metal oxides were also achievable by vaporization and condensation at high temperatures.[2c] It has been found that upon thermal annealing at *elevated* temperatures or by high-energy laser pulses, particles of nonspherical shapes tend to evolve into spherical structures either in solution or in solid state.[11]

As the nanoparticle shape, along with nanoscale dimensions, plays an important role in governing the unique material properties (e.g., optical, electronic, catalytic, etc),[1] studies of the particle shape evolution will provide a mechanistic insight into the manipulation and control of the properties and functions. In this report, we describe a study of novel surface morphological evolutions involving copper nanoparticles. The copper particles were synthesized in a one-phase system with an alkanethiolate protecting monolayer. The fresh samples exhibit material properties that are very similar to those of other alkanethiolate-protected (transition-metal) nanoparticles. For instance, the as-produced particles are mostly of spherical shape and exhibit a Mie scattering profile in optical absorption measurements. Like their noble metal counterparts,[12] these monolayer-protected copper nanoparticles are stable in both solution and dry (airless) forms, in contrast to the "naked" particles with only physisorbed supports.[5] In addition, in solution the particles behave as molecular capacitors, and the corresponding voltammetric measurements reveal rather well-defined quantized capacitance charging features. More interestingly, in solid state these particles are found to undergo surface morphological evolution into varied distinctly faceted crystalline structures upon low-temperature thermal annealing under ambient conditions, where varied particle shapes including hexagons, pentagons, diamonds, triangles, and even rods are observed. This observation is in great contrast to previous studies where thermal annealing typically leads to the formation of nanoparticles of spherical shape.[11] The molecular mechanism for these structural evolutions will be proposed and briefly discussed.

Experimental Section

Chemicals. Copper nitrate ($Cu(NO_3)_2$, Fisher), tetra-*n*-octylammonium bromide (TOABr, 98%, Aldrich), *n*-hexanethiol (C6SH, 96%, ACROS), sodium borohydride ($NaBH_4$, 98+%, Aldrich), and superhydride (lithium triethylborohydride 1.0 M in tetrahydrofuran (THF), Aldrich) were used as received. All solvents were acquired from typical commercial sources and

† Part of the special issue "Royce W. Murray Festschrift".

* Corresponding author. E-mail: schen@chem.siu.edu.

10.1021/jp011280n CCC: $20.00
Published on Web 07/27/2001

used as received as well. Water was supplied by a Barnstead Nanopure Water system (18.3 MΩ).

Particle Synthesis. The particles were synthesized in a one-phase system. In a typical reaction, 1 mmol of $Cu(NO_3)_2$ was dissolved in 4 mL of Nanopure water, into which was added 40 mL of THF with 1.1 g TOABr under vigorous stirring. Then ca. 430 μL (3 mmol) of C6SH was added into the solution where the solution turned somewhat cloudy and became yellowish. Finally, ca. 2 mL of 1.0 M superhydride in THF was added dropwise into the solution and the solution color was found to change rapidly to dark brown. This indicated the formation of *n*-hexanethiolate-protected Cu nanoparticles. 40 mL of toluene and 20 mL of Nanopure water were then introduced into the solution to initiate phase separation. The toluene phase was then collected and, after vigorous stirring in a N_2 atmosphere for 24 h, dried under reduced pressure with a rotary evaporator. Free thiol and TOABr ligands were then removed by rinsing the collected black solids with copious methanol and acetone. The resulting solids were then washed with toluene and filtered with a medium-pore frit to afford purified C6Cu particles in the filtrate, with a typical yield of roughly 30%. This particular sample was labeled C6Cu (rt, 3×) to indicate the synthetic conditions where the reaction was carried out at room temperature with 3-fold excess of thiol over copper. Similarly, copper particles of (rt, 1×) and (rt, 2×) were also synthesized.

The resulting particles were found to be very hydrophobic, soluble in a variety of apolar solvents, including hexane, benzene, toluene, dichloromethane, and chloroform, but not in polar solvents such as alcohols, acetone, and water, similar to other alkanethiolate-protected transition-metal nanoparticles.[12] Proton NMR spectroscopy (Varian 300) was used to examine the purity of the nanoparticles where a concentrated solution of particles was prepared in benzene-d_6. The resulting spectrum showed only a pair of broad peaks at 0.95 and 1.4 ppm corresponding to the methyl and methylene protons, similar to those observed with other alkanethiolate-protected (transition-metal) particles.[12] The absence of sharp NMR signals indicates that the samples are spectroscopically clean.

Spectroscopic Studies. Transmission electron microscopy (Hitachi H7100 at 75 kV) was used to characterize the particle size and size distribution. The samples were prepared by dropcasting the particle solutions in hexane onto a carbon-Formvar or silicon coated nickel grid which was then dried under ambient conditions prior to being introduced into the TEM chamber. Nanoparticle morphological evolution was effected when the same TEM grid was put into a 45 °C oven for a prolonged period of time (~2 months). TEM micrographs at 100k to 300k magnifications were acquired at more than three different spots, from which the particle size distribution was determined. Energy-dispersive X-ray (EDX) analysis (Noran Voyager III EDX analyzer) was carried out to identify the elemental composition of the resulting particles where two strong copper signals were observed at 8.05 and 0.93 keV (see Supporting Information for the EDX spectrum). In addition, selected-area electron diffraction (SAED) was performed to investigate the particle crystalline structures.

UV−vis spectroscopy was carried out with an ATI UNICAM UV4 spectrometer with a 1-cm quartz cuvette. Solutions were prepared typically at a concentration of 0.1 mg/mL in dichloromethane (CH_2Cl_2). FTIR spectra were acquired with a Nicolet FTIR 300 spectrometer with a resolution of 4 cm^{-1}. The samples were prepared by dropcasting the particle solutions in CH_2Cl_2 onto a KBr plate to form a thick film, and further dried in a gentle N_2 stream.

Electrochemistry. Electrochemical studies were carried out with a BAS 100BW electrochemical workstation. A polycrystalline Pt disk (sealed in a glass tubing, area 0.01 cm^2) was used as the working electrode. A Ag/AgCl wire and a Pt coil were used as the (quasi-) reference and counter electrodes, respectively. Prior to use, the Pt working electrode was polished with 0.05 μm Al_2O_3 slurries, and subsequently sonicated in dilute HNO_3, H_2SO_4, and Nanopure water. The electrode was then subjected to electrochemical etching by applying rapid potential sweeping in 0.10 M H_2SO_4 within the potential range of −0.5 to +0.6 V at 10 V/s for 5 min. The electrolyte solution containing Cu nanoparticles was deaerated with high-purity N_2 for at least 20 min, and blanketed with a N_2 atmosphere during the entire experimental procedure.

Results and Discussion

In this section, we first describe transmission electron microscopic studies of alkanethiolate-protected copper nanoparticles and the surface morphological evolutions induced by thermal annealing in solid state. Optical, spectroscopic, and electrochemical characterizations will then be presented for the as-produced nanoparticles.

Transmission Electron Microscopy (TEM). TEM has been a powerful tool in investigating the nanoparticle molecular dimensions and structures.[1−12] Figure 1A and B shows two representative TEM micrographs of the C6Cu (rt, 3×) nanoparticles, with Figure 1C depicting the particle size histogram. One can see that in general the particles exhibit spherical shape (Figure 1A) and more than 65% of the particles fall within the size range of 1.0 to 2.0 nm in diameter (Figure 1C). The mean particle diameter is ca. 1.93 nm with modest dispersity (~35%).

In addition to these well-dispersed small particles, TEM measurements also show the presence of various very large (>15 nm) particles of irregular shape, some of which exhibit very well-defined faceted morphology (Figure 1B). The chain-like features of nearby particles shown in Figure 1B are due to the formation of nanoparticle bilayer structures where the top layer sits at the 2-fold saddle sites between neighboring particles, as observed previously with gold and palladium particles of small size dispersity.[12d]

Selected area electron diffraction (SAED) (Figure 2A) of these particles reveals only diffusive ring patterns, which are most probably attributed to the small particle size and the polycrystalline nature of the particle cores. Nevertheless, the diffraction features were consistent with the fcc crystalline structures of bulk metallic copper, with the two brightest rings corresponding to the diffraction planes of (111) and (220).

However, when the particles were subjected to prolonged low-temperature thermal annealing, interesting nanocrystalline structures were observed. Figure 3A and B shows a pair of representative TEM micrographs of the same CuC6 (rt, 3×) particles after the TEM grid was put into a 45 °C oven for 2 months under ambient conditions. One can see that in addition to the spherical nanometer-sized particles shown in the background (Figure 3A), there is a scattering of much larger (> 10 nm) particles of distinct surface morphologies (please note the difference in scale between (A) and (B)). These can be easily identified as spherical, icosahedron (hexagon), decahedron (pentagon), octahedron (diamond), tetrahedron (triangle), and even rod-shape structures with very well-defined crystalline facets.[13] Previously in reverse micelle microreactors, Pileni et al. observed the formation of copper nanoparticles of varied shapes but with the majority being either spherical or cylindrical,[5] which was partly interpreted by the varied shapes of the

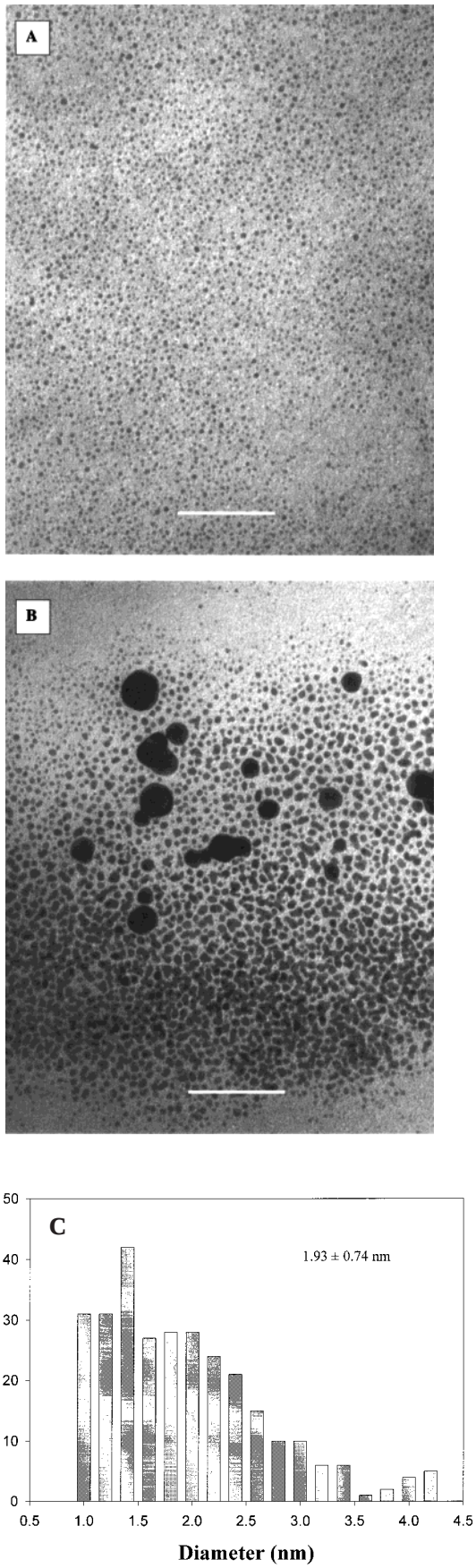

Figure 1. Representative TEM micrographs (A and B) of fresh CuC6 (rt, 3×) particles synthesized with superhydride as the reducing reagent. Scale bars are 51 nm. (C) depicts the particle size histogram.

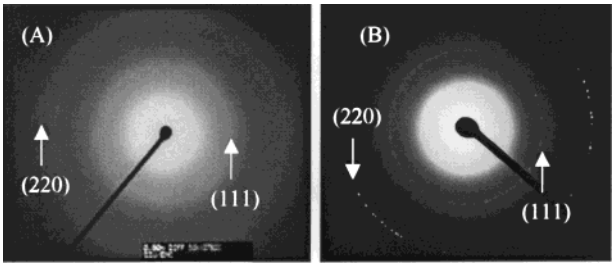

Figure 2. Selected area electron diffraction of the (A) as-produced and (B) thermally annealed CuC6 (rt, 3×) particles.

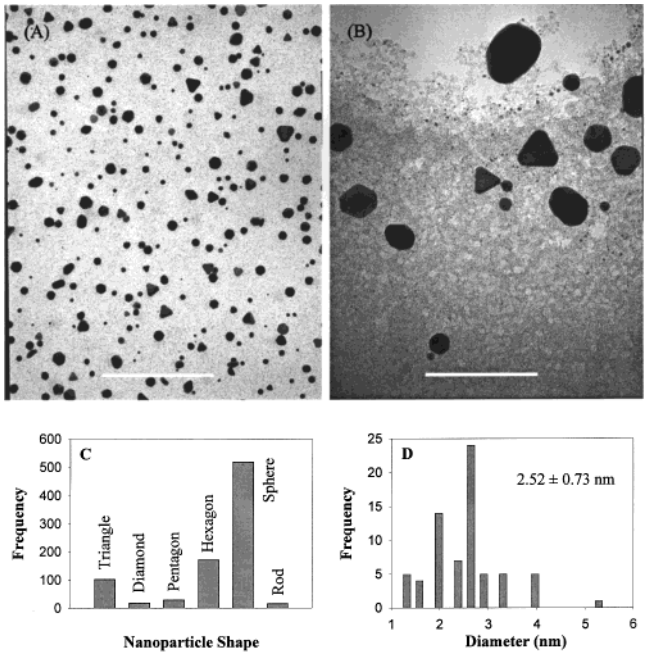

Figure 3. Representative TEM micrographs (A and B) of CuC6 (rt, 3×) particles after prolonged low-temperature thermal annealing. Scale bars (A) 100 nm and (B) 33 nm. (C) depicts the population distribution of particles of varied shapes. (D) shows the size histogram of the small particles exhibited in the background of (A) and (B).

micellar support. This is in contrast to the present observations where the surface morphological evolutions occurred in air without apparent matrix support.

Figure 3C shows the population distribution of these varied shapes, and one can see that the majority (> 50%) of these large particles are of spherical shape. The next most populous shapes are icosahedron (hexagon, ∼20%) and tetrahedron (triangle, ∼10%), with the rest being of octahedron (diamond), decahedron (pentagon), and rod shaped structures. The typical dimensions of these varied-shaped nanocrystals range from 10 to 40 nm with 20 to 50% dispersity (see Supporting Information for their size distributions). Of these, spherical particles are the most disperse with the average diameter of 16.33 and 8.11 nm standard deviation (50%). Nanocrystals of other shapes are somewhat larger (> 20 nm) and less disperse (<30%). For octahedron (diamond) and rod shaped structures, the aspect ratios were found to be about 1.2−1.5 (the long and short axes are indicated in the respective inset cartoons), much smaller than that of copper nanocylinders synthesized in reverse micelles.[5]

Corresponding electron diffraction demonstrated some spotty ring patterns (Figure 2B) indicating well-defined crystalline lattices, which were consistent with those of bulk copper oxide (Cu_2O) instead of metallic copper. The two brightest rings are indexed to the (111) and (220) diffraction of Cu_2O. In addition,

overall the particle dimension was found to be somewhat larger than that of the as-produced particles. Figure 3D depicts the histrogram of the small particles shown in the background of Figure 3B, and the average size is found to be 2.52 ± 0.73 nm. This indicates a roughly 30% increase of the particle diameter after thermal annealing. This cannot be explained solely by the expansion of crystal lattice when metallic copper is oxidized into copper oxide, as the fcc crystal lattice for Cu_2O (0.425 nm) is only about 18% larger than that for Cu metal (0.361 nm).[14] Additional contribution is most likely attributed to the sacrifice of smaller particles in the formation of "jumbo" nanocrystals, akin to solution-phase Oswald ripening.

Whereas the detailed molecular mechanism is not clear at the moment for the formation of these "jumbo" nanocrystals of distinct shapes, it is quite possible that these much larger, well-faceted nanocrystals are mainly generated simply by low-temperature thermal annealing of the original irregular-shaped particles (for instance, see Figure 1B). Additional contributions to the formation of these morphologically well-defined nanocrystals might be from the particle aggregates (such as the bilayered chains observed in Figure 1B) where the molecular mechanism might involve the oxidation of copper cores and the consequential desorption of alkanethiolates leading to the fusion of stacking particles. One supporting observation is that after thermal annealing the particle concentration (or density) on the TEM grid was much lower (e.g., Figure 3B vs Figure 1A) where no chain structures of particles were found.

Spectroscopic Studies. Nanosized particles exhibit unique optical properties with an exponential-decay Mie scattering profile with decreasing photon energy. Some transition-metal nanoparticles also show a distinct surface-plasmon band. For instance, nanosized Cu particles typically exhibit a surface-plasmon peak at around 566 nm.[15] However, for the fresh copper nanoparticles synthesized here, the corresponding UV−vis absorption spectrum (see the Supporting Information) only demonstrates a featureless Mie scattering profile without the appearance of an apparent surface-plasmon band. This might be, at least in part, attributed to the small particle size (<2 nm), as the surface-plasmon peak is known to be broadened and depressed with decreasing particle size.[16]

FTIR spectroscopy has been used previously to examine the conformational structure of the particle-bound organic surfactant monolayers, where the energies of the symmetric (d^+) and antisymmetric (d^-) stretching vibrations of the methylene units are taken as a sensitive diagnostic indicator for the ordering of the adsorbed alkanethiolate molecules.[12b] Using dropcast thick films of the above-obtained CuC6 particles, these two bands were observed at (d^-) 2924.50 and (d^+) 2855.62 cm^{-1}, respectively. In comparison, in crystalline polyethylene these two vibrational modes are found at 2920 and 2850 cm^{-1}, whereas in solution they become 2928 and 2856 cm^{-1}.[12b] Thus, one can see that the Cu particle-bound hexanethiolate monolayers resemble the liquid state structure, presumably with a high density of gauche defects. This is consistent with previous observations with other transition metal nanoparticles.[12]

Electrochemistry. Alkanethiolate-protected nanoparticles behave as molecular capacitors in solutions, which is manifested by the electrochemical Coulomb staircase characteristics.[17] For instance, these quantized charging features have been observed previously with monolayer-protected gold and palladium nanoparticles.[12b,d] Here we also carried out electrochemical investigations of these nanosized copper particles. Figure 4A shows the corresponding differential pulse voltammogram (DPV) of the fresh C6Cu nanoparticles dissolved in CH_2Cl_2 containing 0.10 M TBAP as the supporting electrolyte. One can see that there are multiple voltammetric peaks within the potential range of −0.6 to +0.8 V (vs Ag/AgCl), with each peak corresponding to a single-electron-transfer event (each peak identified with an asterisk).[17] Considering that the particles are unfractionated, the results are quite remarkable.

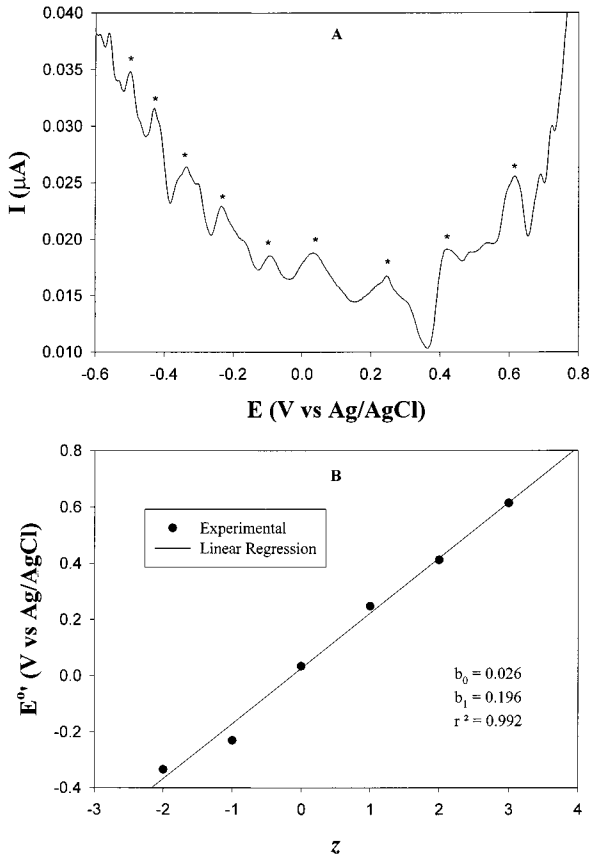

Figure 4. (A) Differential pulse voltammogram (DPV) of the as-produced CuC6 (rt, 3×) nanoparticles at a platinum disk electrode in 0.10 M TBAP in CH_2Cl_2. The particle concentration was ca. 3 mg/mL. Platinum electrode area 0.01 cm^2. DC ramp was 10 mV/s, pulse amplitude 50 mV. (B) Variation of formal potential ($E^{o\prime}_{z,z-1}$) of the charging peaks with particle charge state (z). Symbols are experimental data and line is the linear regression.

It has been found that the formal potentials ($E^{o\prime}_{z,z-1}$) of the charging peaks are related to the particle charge state (z),[17c] $E^{o\prime}_{z,z-1} = E_{PZC} + ((z - (1/2))e/C_{MPC})$, where E_{PZC} is the particle potential of zero charge, C_{MPC} is the particle molecular capacitance, and e is electronic charge. Figure 4B depicts the variation of formal potential with particle charge state, which shows a very good linear relationship (within the potential range of −0.4 to +0.6 V). From the linear regression, one can evaluate the molecular capacitance of the C6Cu particles, $C_{MPC} = 0.82$ aF. Assuming a concentric structural model of the monolayer-protected nanoparticles,[17c] this corresponds to an effective dielectric constant of 3.2 for the copper core-supported alkanethiolate monolayers. This dielectric value is similar to that found with gold nanoparticle-bound alkanethiolate self-assembled monolayers.[17c]

It should be noted that aged particles typically fail to reveal the discrete electron-transfer features, especially after prolonged exposure to air, presumably due to the oxidation of the copper core. The resulting featureless voltammetric responses are more like the so-called Coulomb blockade, a behavior characteristic of the band gap structure of semiconductor materials.[18]

Conclusion

Alkanethiolate-protected copper nanoparticles were synthesized in a one-phase system. The as-produced particles were mostly of spherical shape; however, after prolonged low-temperature thermal annealing under ambient conditions, distinct morphological evolution was observed where well-defined faceted nanocrystals were found in varied geometric shapes. This was attributed to the oxidation of copper cores into crystalline copper oxide as well as the Oswald-ripening-like behavior of smaller particles in solid state.[19] Further studies will be carried out to examine the effects of particle size and monolayer properties on the nanocrystal morphological evolutions. These might be of technological importance in the understanding and manipulation of the catalytic activities of copper nanoparticles in solid state.

Spectroscopic studies of the fresh copper particles exhibited a Mie-scattering profile without the appearance of a well-defined surface plasmon band, most probably due to the small particle size. Electrochemical investigations of the as-produced particles revealed quantized charging features where the particle molecular capacitance was evaluated; in contrast, aged particles exhibited voltammetric features that were similar to those observed with semiconductor materials.

Acknowledgment. The authors are grateful for Ms. L. A. Truax's technical assistance in the early stage of the experiment. J.M.S. thanks the SIU Department of Chemistry for an Undergraduate Summer Research Fellowship. This work was supported in part by the Office of Naval Research, the National Science Foundation (CAREER Award), the Petroleum Research Fund administered by the American Chemical Society, the Illinois Department of Commerce and Community Affairs, and the SIU Materials Technology Center. S.C. is a Cottrell Scholar of Research Corporation.

Supporting Information Available: EDX and UV−vis spectra of the hexanethiolate-protected copper nanoparticles. Size distribution of the copper particles of varied shapes. These materials are available free of charge via the Internet at http://pubs.acs.org.

References and Notes

(1) Schmid, G. *Clusters and Colloids: From Theory to Applications*, VCH: New York, 1994. (b) Haberland, H., Ed. *Clusters of Atoms and Molecules*; Springer-Verlag: New York, 1994. (c) Turton, R. *The Quantum Dot: A Journey into the Future of Microelectronics*; Oxford University Press: New York, 1995. (d) Hayat, M. A., Ed. *Colloidal Gold: Principles, Methods, and Applications*; Academic Press: New York, 1989; Vol. 1.

(2) Ahmadi, T. S.; Wang, Z. L.; Green, T. C.; Henglein, A.; El-Sayed, M. A. *Science* **1996**, *272*, 1924. (b) Wang, Z. L. *J. Phys. Chem. B* **2000**, *104*, 1153. (c) Pan, Z. W.; Dai, Z. R.; Wang, Z. L. *Science* **2001**, *291*, 1947.

(3) Torigoe, K.; Esumi, K. *Langmuir* **1995**, *11*, 4199.

(4) Bradley, J. S.; Tesche, B.; Busser, W.; Maase, M.; Reetz, M. T. *J. Am. Chem. Soc.* **2000**, *122*, 4631.

(5) Tanori, J.; Pileni, M. P. *Langmuir* **1997**, *13*, 639. (b) Pileni, M. P.; Gulik-Krzywicki, T.; Tanori, J.; Filankembo, A.; Dedieu, J. C. *Langmuir* **1998**, *14*, 7359.

(6) Crooks, R. M., Zhao, M.; Sun, L.; Chechik, V.; Yeung, L. K. *Acc. Chem. Res*. **2001**, *34*, 181. (b) Balogh, L.; Tomalia, D. A. *J. Am. Chem. Soc*. **1998**, *120*, 7355.

(7) Puntes, V. F.; Krishnan, K. M.; Alivisatos, A. P. *Science* **2001**, *291*, 2115.

(8) Lu, D.-L.; Tanaka, K. *J. Phys. Chem. B* **1997**, *101*, 4030.

(9) Yu, Y.; Chang, S.; Lee, C.; Wang, C. R. C. *J. Phys. Chem. B* **1997**, *101*, 6661. (b) Mohamed, M. B.; Ismail, K. Z.; Link, S.; El-Sayed, M. A. *J. Phys. Chem. B* **1998**, *102*, 9370.

(10) Martin, C. R. *Chem. Mater*. **1996**, *8*, 1739. (b) Martin, B. R.; Dermody, D. J.; Reiss, B. D.; Fang, M.; Lyon, L. A.; Natan, M. J.; Mallouk, T. E. *Adv. Mater*. **1999**, *11*, 1021.

(11) Hulteen, J. C.; Patrissi, C. J; Miner, D. L.; Crosthwait, E. R.; Oberhauser, E. B.; Martin, C. R. *J. Phys. Chem. B* **1997**, *101*, 7727. (b) Lisiecki, I.; Sack-Kongehl, H.; Weiss, K.; Urban, J.; Pileni, M. P. *Langmuir* **2000**, *16*, 8802 and 8807. (c) Maye, M. M.; Zheng, W.; Leibowitz, F. L.; Ly, N. K.; Zhong, C. J. *Langmuir* **2000**, *16*, 490. (d) El-Sayed, M. A. *Acc. Chem. Res*. **2001**, *34*, 257.

(12) Brust, M.; Walker, M.; Bethell, D.; Schiffrin, D. J.; Whyman, M. *J. Chem. Soc., Chem. Comm*. **1994**, 801. (b) Templeton, A. C.; Wuelfin, W. P.; Murray, R. W. *Acc. Chem. Res.* **2000**, *33*, 27. (c) Whetten, R. L.; Shafigullin, M. N.; Khoury, J. T.; Schaaff, T. G.; Vezmar, I.; Alvarez, M. M.; Wilkinson, A. *Acc. Chem. Res*. **1999**, *32*, 397. (d) Chen, S.; Huang, K.; Stearns, J. A. *Chem. Mater*. **2000**, *12*, 540.

(13) The geometrical shapes of the nanocrystals are deduced based on the TEM images of the 2-dimensional cross sections of the particles.[2b]

(14) Lide, D. R., Ed. *CRC Handbook of Chemistry and Physics*, 76th ed., CRC Press: Boca Raton, 1995.

(15) Creighton, J. A.; Eadon, D. G. *J. Chem. Soc., Faraday Trans.* **1991**, *87*, 3881.

(16) Bohren, C. F.; Huffman, D. R. *Absorption and Scattering of Light by Small Particles*; John Wiley & Sons: New York, 1983. (b) Particles synthesized in the same protocol but with varied experimental conditions, e.g., (rt, 1×), (rt, 2×), and (rt, 3×), showed very similar absorption profiles, suggesting a small variation of the particle core sizes (Figure S3 in the Supporting Information).

(17) Ingram, R. S.; Hostetler, M. J.; Murray, R. W.; Schaaff, T. G.; Khoury, J.; Whetten, R. L.; Bigioni, T. P.; Guthrie, D. K.; First, P. N. *J. Am. Chem. Soc*. **1997**, *119*, 9279. (b) Chen, S.; Ingram, R. S.; Hostetler, M. J.; Pietron, J. J.; Murray, R. W.; Schaaff, T. G.; Khoury, J. T.; Alvarez, M. M.; Whetten, R. L. *Science* **1998**, *280*, 2098. (c) Chen, S.; Murray, R. W.; Feldberg, S. W. *J. Phys. Chem. B* **1998,** *102*, 9898.

(18) Chen, S.; Truax, L. A.; Sommers, J. M. *Chem. Mater*. **2000**, *12*, 3864.

(19) In another approach, we produced the copper particles using a two-phase system akin to that developed by Brust et al.[12a] with $NaBH_4$ as the reducing reagent. The resulting particles tended to be somewhat smaller than those obtained in the one-phase approach using superhydride as the reducing agent. Both approaches appeared to generate rather stable alkanethiolate-protected copper nanoparticles.